PROCEEDINGS OF SCIENCE

Dual-frequency EVN Observations of a Large Sample of Distant Radio Quasars

Máté Krezinger,[a,b,*] **Krisztina Perger,**[b] **Krisztina É. Gabányi,**[a,b,c] **Sándor Frey,**[b,d] **Leonid I. Gurvits,**[e,f] **Zsolt Paragi,**[e] **Tao An,**[g] **Yingkang Zhang,**[g] **Hongmin Cao**[h] **and Tullia Sbarrato**[i]

[a] *Department of Astronomy, Institute of Geography and Earth Sciences, ELTE Eötvös Loránd University, Pázmány Péter sétány 1/A, H-1117 Budapest, Hungary*

[b] *Konkoly Observatory, ELKH Research Centre for Astronomy and Earth Sciences, Konkoly Thege Miklós út 15-17, H-1121 Budapest, Hungary*

[c] *ELKH-ELTE Extragalactic Astrophysics Research Group, ELTE Eötvös Loránd University, Pázmány Péter sétány 1/A, H-1117 Budapest, Hungary*

[d] *Institute of Physics, ELTE Eötvös Loránd University, Pázmány Péter sétány 1/A, H-1117 Budapest, Hungary*

[e] *Joint Institute for VLBI ERIC, Oude Hoogeveensedijk 4, 7991 PD Dwingeloo, The Netherlands*

[f] *Department of Astrodynamics and Space Missions, Delft University of Technology, Kluyverweg 1, 2629 HS Delft, The Netherlands*

[g] *Shanghai Astronomical Observatory, Key Laboratory of Radio Astronomy, Chinese Academy of Sciences, 80 Nandan Road, Shanghai 200030, China*

[h] *School of Physics and Electrical Information, Shangqiu Normal University, 298 Wenhua Road, Shangqiu, Henan 476000, China*

[i] *INAF – Osservatorio Astronomico di Brera, via E. Bianchi 46, I-23807 Merate, Italy*

E-mail: krezinger.mate@csfk.org

Milliarcsecond-scale observations of high-redshift radio quasars provide unique insight to jet structure, formation and evolution. To date, only a handful of already known high-redshift ($z > 4$) radio quasars had been imaged with very long baseline interferometry (VLBI). To substantially increase the sample available for studying the population of high-redshift radio-loud active galactic nuclei, we selected 13 radio quasars for imaging with the European VLBI Network (EVN) at 1.7 and 5 GHz. Here we present the preliminary analysis of the experiment lasting for almost three years, by investigating the spectral characteristics, morphology and brightness temperature of the sources. Compact radio emission was detected in all objects. Our results indicate that about half of the sample consists of unbeamed radio sources, some of which show significant offset between the optical and radio positions.

**** European VLBI Network Mini-Symposium and Users' Meeting (EVN2021) ****
**** 12-14 July, 2021 ****
**** Online ****

[*] Speaker

PoS(EVN2021)008

1. Introduction

High-redshift quasars hold one key to understand the evolution of galaxies and supermassive black holes in the early Universe ($z > 4$), as the observations of the distant quasars could provide information from early-time star forming activity to active galactic nuclei (AGN). The latter are powered by accretion of supermassive black holes (SMBH) with masses of already up to $10^{10} M_{\odot}$ [8]. The increment of the number of high-z radio sources, resulted from the efforts of searching for high-z quasars, provides a chance to investigate the early-time jet activities [8]. The number of the misaligned radio quasars at $z > 3$, deduced from the blazar sample in the same redshift interval, seems to be more than that observed [11], while high-resolution milliarcsecond (mas) scale observations of blazar candidates – identified via X-ray observations – reveal some extended, or even symmetric radio structures with steep spectra [2–4]. This indicates that there are misaligned sources misclassified as blazars. For blazars, we expect to find compact radio cores with flat spectrum and Doppler-boosted emission. With very long baseline interferometry (VLBI), we can classify the already known high-redshift radio sources more definitively, since it can distinguish between a compact core and a more extended radio emission. Studying and classifying the high-redshift sources might help to understand why many misaligned sources are actually "missing". In addition to the VLBI observations, the recent *Gaia* Early Data Release 3 (EDR3) optical astrometric positions [5] also help in the classification process. The optical position is related to the accretion disk around the SMBH, while the VLBI position points to the brightest and most compact radio emission in the jet. In some cases, when there is bright, pc-scale optical synchrotron jet emission present, the optical position may be offset by up to a few mas along the VLBI jet direction (e.g. [6]). Determining the angular separation between the two positions can also help to decide whether the sources are compact symmetric objects (CSOs) or core–jet type objects.

2. Sample and observations

We selected thirteen $4 < z < 4.5$ radio quasars from the list of Sbarrato et al. [9] list which have not yet been imaged with VLBI. They represent radio AGN at similar cosmological distances, and they are selected as blazars candidates because of their high radio loudnesses. With only a few dozens of radio quasars at $z > 4$ imaged with VLBI to date, these quasars increase the sample substantially, by about 25%. They are all detected in the 1.4 GHz Very Large Array (VLA) Faint Images of the Radio Sky at Twenty-centimeters (FIRST) survey [12], with flux densities in the range $\sim 1 - 100$ mJy. We performed phase-referenced VLBI observations with the EVN at two frequencies, 1.7 and 5 GHz, during several observing epochs between 2017 December and 2020 November. Most observing networks included long east–west baselines. In addition to the elements of the EVN, e-MERLIN antennas were occasionally also included.

We used AIPS [7] for the initial data calibration, then DIFMAP [10] for imaging. In DIFMAP, we applied the CLEAN deconvolution algorithm and when the source flux densities exceeded 15 mJy, phase self-calibration was also performed. Circular Gaussian model components were fitted to the calibrated visibility data to characterize the brightness distribution of the sources. A detailed description of the observations and data analysis will be presented elsewhere (Krezinger et al., in prep.).

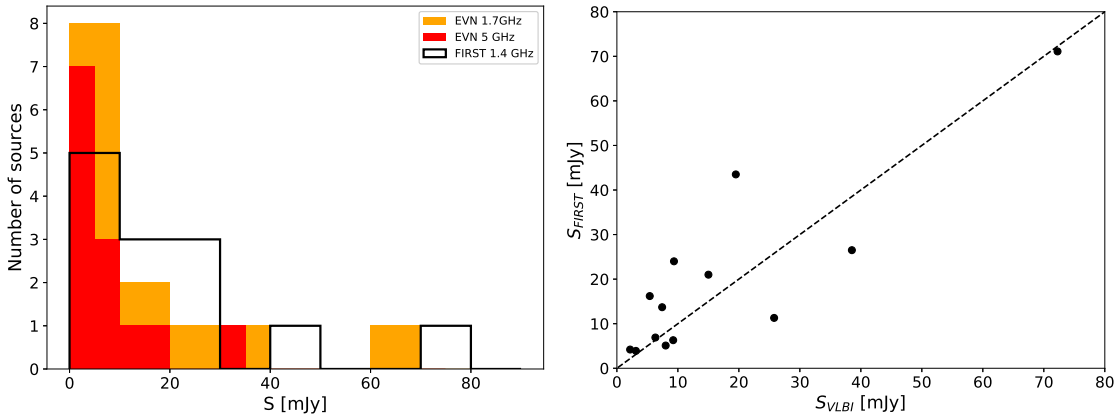

Figure 1: *Left:* Histograms of the flux density distribution of the target sources. Open columns with black outline: FIRST 1.4 GHz flux densities. Orange: EVN 1.7 GHz flux densities. Red: EVN 5 GHz flux densities. *Right:* FIRST 1.4 GHz flux density vs. VLBI flux density extrapolated to the same fequency from 1.7 GHz. The error bars are comparable to or smaller than the symbol size. The measurements were non-simultaneous, the sources located below the dashed line are certainly variable because the flux density in their mas-scale structure appears higher than the total value measured in FIRST at another epoch.

The left panel of Fig. 1 shows the FIRST and the EVN flux density distributions of the target sources. The latter values are determined by model fitting. Our VLBI data provide essential information on the source compactness, brightness temperatures and spectral properties. Furthermore, the flux densities can be compared to previous low-resolution radio measurements to look for possible variability (Fig. 1, right). In the following, we present two examples of the target sources, then draw a preliminary conclusion for the whole sample.

3. Results

3.1 J1006+4627

J1006+4627 is a blazar-like source with compact radio emission associated with a flat spectrum ($\alpha = -0.25 \pm 0.11$; the spectral index is defined as $S \propto \nu^{\alpha}$, where S is flux density and ν is frequency) and moderate brightness temperature. The 1.7 GHz image (Fig. 2, left) shows a slightly extended emission towards the east of the central component. Variability can also be deduced from the measured EVN flux densities that are above the historic low-resolution values. The *Gaia* position of this source shows an eastward offset from the VLBI one within 3 mas which may be significant. The bright VLBI component at the centre detected with the EVN might be a compact core, the base of the advancing jet. The calibrator was J0958+4725, a bright quasar with simple structure.

3.2 J1520+1835

One of the most interesting targets in the sample is J1520+1835 (the phase-reference calibrator source was J1521+1756). By looking at the EVN images, we can see a rather compact feature at both frequencies (the 1.7 GHz image is displayed in the right panel of Fig. 2). However, there is no indication of Doppler-boosted emission, flat spectrum or variability. On the contrary, this

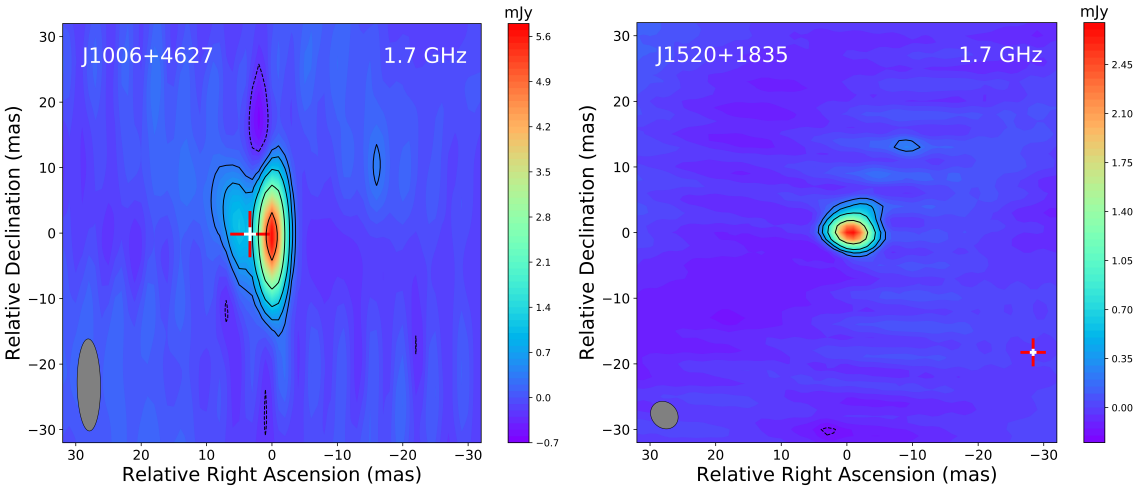

Figure 2: Naturally weighted 1.7 GHz EVN CLEAN images of J1006+4627 and J1520+1835. The red and white cross marks the *Gaia* position, where the white part indicates the formal uncertainties. The grey ellipses at the bottom-left corners represent the Gaussian restoring beams. *Left (J1006+4627)*: The peak intensity is 5.72 mJy beam^{-1}. The lowest contours are drawn at ±0.3 mJy beam^{-1}, the positive contour levels increase by a factor of 2. The half-power beam width (HPBW) is 14.1 mas × 3.6 mas with a position angle PA = 0.8° measured from north through east. *Right (J1520+1835)*: The peak intensity is 0.66 mJy beam^{-1}. The lowest contours are drawn at ±0.08 mJy beam^{-1}. The HPBW is 7.4 mas × 1.4 mas with PA = 88.3°.

source has $\alpha = -1.42 \pm 0.21$, an ultra steep spectrum commonly found in young radio sources. Another unusual property is the location of the *Gaia* optical position. The optical source is found ∼ 30 mas away from the VLBI position towards southwest, the separation corresponds to ∼ 250 pc projected linear offset at redshift $z = 4.12$. CSOs known to be the youngest jetted AGNs [1] typically have similar separations between their radio lobes and the core, the latter often being invisible in radio. The measured offset supports the young radio source scenario for J1520+1835. The radio emission detected with the EVN may originate from a compact hot spot inside a radio lobe, while the measurements were not sensitive enough to detect the fainter lobe on the other side of the central object that coincides with the *Gaia* optical source. J1520+1835 would be a good target for a follow-up e-MERLIN observation to check for extended radio emission in the vicinity of the VLBI component.

3.3 Preliminary findings for the whole sample

All 13 targets in our project were successfully detected with EVN at both frequencies. Using the model parameters fitted to the visibility data, we derived their brightness temperatures and monochromatic radio powers. We were also able to determine the two-point spectral index between 1.7 and 5 GHz for the compact structure for 11 sources: 6 of them show flat and 5 show steep spectra. (For the remaining two sources, we cannot rely on the 5 GHz amplitude calibration due to technical reasons.) The *Gaia* EDR3 optical positions coincide with the 5 GHz radio positions for most of our sources. We also compared our EVN measurements with low-resolution flux densities available in the literature, enabling us to investigate the continuum radio spectra. More details about the physical parameters of these objects will be presented in Krezinger et al. (in prep.). Roughly

half of the sources are blazar-like objects with compact core–jet structures and flat spectrum, while the rest are unbeamed gigahertz-peaked spectrum sources or CSOs.

Acknowledgements: The EVN is a joint facility of independent European, African, Asian and North American radio astronomy institutes. Scientific results from data presented in this publication are derived from the following EVN project code: EG102. e-MERLIN is a National Facility operated by the University of Manchester at Jodrell Bank Observatory on behalf of STFC. The research leading to these results has received funding from the European Commission Horizon 2020 Research and Innovation Programme under grant agreement No. 730562 (RadioNet). We thank the Hungarian National Research, Development and Innovation Office (OTKA K134213 and 2018-2.1.14-TÉT-CN-2018-0001) for support.

References

[1] An, T., Baan, W.A. 2012, ApJ, 760, 77. doi:10.1088/0004-637X/760/1/77

[2] Cao, H.-M., Frey, S., Gabányi, K. É., et al. 2017, MNRAS, 467, 950. doi:10.1093/mnras/stx160

[3] Coppejans, R., Frey, S., Cseh, D., et al. 2016, MNRAS, 463, 3260. doi:10.1093/mnras/stw2236

[4] Gabányi, K. É., Frey, S., An, T., et al. 2021, Astronomische Nachrichten, 342, 1092. doi:10.1002/asna.20210057

[5] Gaia Collaboration, Brown, A.G.A., Vallenari, A., Prusti, T., et al. 2021, A&A, 649, A1. doi:10.1051/0004-6361/202039657

[6] Kovalev, Y. Y., Petrov, L., & Plavin, A. V. 2017, A&A, 598, L1. doi:10.1051/0004-6361/201630031

[7] Greisen, E. W. 2003, in: Information Handling in Astronomy – Historical Vistas, ed. Heck, A., Astrophysics and Space Science Library, 285, 109. doi:10.1007/0-306-48080-8_7

[8] Sbarrato, T. 2021, Galaxies, 9, 23. doi:10.3390/galaxies9020023

[9] Sbarrato, T., Ghisellini, G., Nardini, M., et al. 2013, MNRAS, 433, 2182. doi:10.1093/mnras/stt882

[10] Shepherd, M. C. 1997, in: Astronomical Data Analysis Software and Systems VI, eds. Hunt, G., Payne, H.E., ASP Conference Series, 125, 77

[11] Volonteri, M., Haardt, F., Ghisellini, G., et al. 2011, MNRAS, 416, 216. doi:10.1111/j.1365-2966.2011.19024.x

[12] White, R. L., Becker, R. H., Helfand, D. J., et al. 1997, ApJ, 475, 479. doi:10.1086/303564